Therapeutic peptides targeting the Ras superfamily

Journal:	*Peptide Science*
Manuscript ID	PEP-2020-01-00005.R1
Wiley - Manuscript type:	Review
Date Submitted by the Author:	25-Mar-2020
Complete List of Authors:	Hurd, Catherine; University of Cambridge, Biochemistry Mott, Helen; University of Cambridge, Biochemistry Owen, Darerca; University of Cambridge, Biochemistry
Keywords:	Cancer, Peptide, GTPase, Ras, Macrocycle

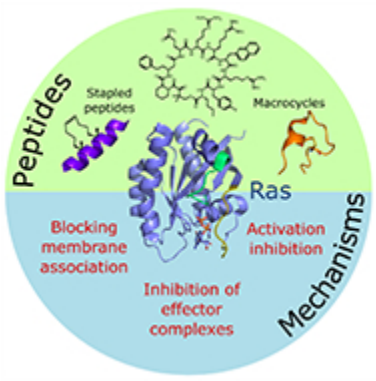

Graphical Abstract

16x16mm (300 x 300 DPI)

Therapeutic peptides targeting the Ras superfamily

Catherine A. Hurd, Helen R. Mott and Darerca Owen*

Department of Biochemistry, University of Cambridge, 80 Tennis Court Road, Cambridge.

*To whom correspondence should be addressed.

Abstract

The Ras superfamily of small GTPases are master regulators of numerous essential processes within the cell, so that when they malfunction, cancer and many other diseases can result. For example, activating Ras mutations are present in approximately 20% of human cancers. As such, they are key therapeutic targets, yet more than three decades of intensive research efforts have failed to produce effective Ras inhibitors in the clinic. This is, in part, due to their relatively smooth surfaces which are difficult to target through traditional drug discovery methods using small molecules. Peptides offer a solution to this issue as they occupy larger surface areas on their targets and therefore offer exquisite selectivity and affinity. However, their use in the past has been limited to extracellular targets due to delivery issues. Recent advances in peptide macrocyclization, modifications and delivery methods have ignited increased interest in the use of these highly effective biologics for intracellular targets. This review will cover progress made in the development of peptides targeting small GTPases to treat a wide range of diseases.

1 Introduction

There are more than 150 small GTPases in humans comprising the Ras superfamily, which is divided into Ras, Rho, Rab, Ran and Arf families based on sequence homology and physiological function (Figure 1A). The Ras (Rat sarcoma) family regulates cell proliferation and survival, Rho (Ras homologous) family members are master regulators of actin cytoskeletal rearrangement and cell motility, Rab (Ras-like in brain) proteins regulate membrane trafficking, Ran (Ras-like nuclear) is involved with nucleocytoplasmic transport and Arf (ADP ribosylation factors) proteins regulate vesicle trafficking.[1]

All small GTPases share a conserved G domain of ~20 kDa which binds the guanine nucleotides GDP and GTP with high affinity, involving coordination of a magnesium cation. These proteins exist in two conformationally distinct states: they are inactive when bound to GDP and active in the GTP-bound state where they are competent to bind downstream effectors (Figure 1B). Conformational differences between the two states are greatest in the two flexible regions termed switch I (Ras numbering 30-38) and switch II (residues 59-67): most effector and regulatory proteins bind to one or both of these regions to sense the nucleotide status of the protein. Small GTPases have the potential to hydrolyse GTP to GDP rendering them inactive but intrinsic rates of hydrolysis are very slow, as is the exchange of GDP for GTP. Signalling is therefore negatively regulated by GTPase Activating Proteins (GAPs), which aid hydrolysis of GTP to GDP, while activation is controlled by another set of proteins known as Guanine nucleotide Exchange Factors (GEFs), which assist replacement of GDP for GTP. The majority of Ras superfamily members are modified by a prenyl group, which, often in conjunction with a second membrane-anchoring signal, targets them to specific cellular membranes, with this membrane localization being essential for their activity. In addition to GEFs and GAPs, the Ras, Rho and Rab proteins are negatively regulated by Guanine

nucleotide Dissociation Inhibitors (GDIs) and GDI-like proteins, which promote cytosolic localization by binding and masking the prenyl group modifications.

As these proteins regulate many vital cellular processes, their aberrant signalling can have disastrous consequences and they are heavily implicated in a variety of human diseases including cancer,[2,3] vascular diseases[4] and immune disorders.[5] Although they are highly desirable drug targets, several features of small GTPases make them difficult to target through traditional methods of drug discovery, leading them to be previously considered 'undruggable'. In contrast to the success that has been attained with ATP-competitive inhibitors for kinases, the picomolar affinity exhibited by small GTPases for their nucleotides, along with intracellular GTP concentrations of ~1 mM, makes the nucleotide binding site of these proteins an intractable target for competitive inhibitors.

Inhibition of membrane association to block GTPase signalling has been explored. Early attempts to disrupt Ras signalling used farnesyltransferase inhibitors (FTIs) to block prenylation of the Ras C-terminus and hence the membrane association that is required for transformation.[6] Unfortunately, FTIs failed in clinical trials and it was later discovered that KRas and NRas proteins, the isoforms most commonly mutated in human cancers, can undergo alternative prenylation by Geranylgeranyltransferase (GGTase) I in the presence of FTIs.[7] Dual inhibition of both these enzymes is not expected to be feasible due to their large number of targets, which is likely to lead to toxic side effects. Recently however, Novotny *et al.* have reported a novel method to mislocalize KRas by developing neo-substrates of farnesyltransferase, which modify KRas at the Cys sidechain that is normally farnesylated. This modification prevented further processing and membrane attachment, resulting in cytoplasmic localization of KRas.[8] This approach circumvents issues previously seen with FTIs (which are competitive inhibitors of farnesylation) as the modified KRas cannot be prenylated by GGTase I, offering a promising new avenue to target Ras signalling. Further, unlike the other Ras isoforms, HRas cannot undergo alternative prenylation by GGTase I[7] and could be targeted by competitive FTIs. Indeed, FTIs to target HRas-mutant cancers are currently being investigated in the clinic.[9,10]

Disruption of GTPase interactions with effector proteins has proven challenging as these conventional protein-protein interactions (PPIs) are mediated by relatively large, smooth surfaces that generally lack distinct binding pockets for small molecules. There has however been some recent success generating small molecule inhibitors of Ras, as Shokat and colleagues identified a small pocket beneath switch II which they were able to exploit to generate covalent inhibitors targeting the $KRas^{G12C}$ mutant.[11] This has renewed the hope of using small molecules to inhibit small GTPases, although identification of similar binding pockets on other family members could prove very challenging. The advantage of covalent inhibitors is that compounds with lower affinity are still effective, meaning less well-defined binding pockets are required. Their application is limited however to reactive residues at therapeutically relevant sites, for example the rare mutants that result in an exposed cysteine residue.

Peptides offer an enticing opportunity for the inhibition of PPIs as they offer excellent selectivity and target binding affinity, even at relatively smooth protein surfaces, due to the large area that they occupy. In this way they retain many of the advantages of larger biologics, while their smaller molecular weight enables the possibility of cell entry. Initially peptides were limited to extracellular targets, however developments in the use of cell-penetrating peptides and research into the intrinsic properties that invoke cell uptake have opened up the peptide druggable space to encompass intracellular proteins such as the small GTPases.

Macrocyclization of peptides is one strategy that has been employed for targeting intracellular proteins (for a recent review see [12]). Small cyclic peptides are typically resistant to proteases and have higher target affinities due to their reduced conformational freedom. Several cell-permeable cyclic peptides exist in nature, including the immunosuppressant cyclosporin A, which is also endowed with oral bioavailability, a property that has proven elusive to peptide chemists. Investigation into how these natural products achieve cell entry has been an active area of research (reviewed in [13]) and has guided improvements in cellular permeability of synthetic peptides, for example by N-methylation of amide bonds.[14,15] Some groups now also incorporate cell-permeable peptide (CPP) scaffolds as part of library design,[16] thus eliminating effort spent on hits that cannot be converted to cell penetrant analogues and to eliminate the need to append bulky and often toxic CPPs.

Macrocyclic binders are often derived from *de novo* peptide libraries, however an alternative strategy involves mimicking existing binding motifs from PPI interfaces. Analysis of available Protein Data Bank (PDB) structures revealed that more than 60% of known PPIs contain a helix in the interaction interface,[17] therefore mimicry of this critical binding motif presents an opportunity for inhibitor design. However, when helical peptide sequences are isolated from larger proteins, they often lose secondary structure and so stabilization of α-helical peptides has emerged as an elegant chemical solution to generate rigid, high affinity peptides with improved drug-like properties. The most commonly used example of α-helix stabilization is the all-hydrocarbon staple introduced by Verdine and colleagues.[18] This approach utilises olefin-containing amino acids of appropriate lengths at either *i*, *i* + 4 or *i*, *i* +7 positions of a peptide, which are then covalently linked by a Grubbs ring closing metathesis, though many other strategies exist and have been reviewed recently.[19,20] With careful staple positioning, the stabilized helical structures can have improved affinity due to a reduced entropic penalty upon binding, while in certain instances the staple itself can also interact favourably with the target protein.[21] The incorporation of unnatural amino acids and increased secondary structure often improve the proteolytic stability of the peptides and can also facilitate cell permeability.[22,23] Many peptides have been designed to disrupt GTPase effector or regulator interactions (Table 1) and these will be discussed in detail in this review.

Table 1. Peptides targeting the Ras superfamily of small GTPases

Ras family	Interaction(s) targeted	Peptide name	Structure class	Identified from	Ref
Ras	$KRas^{G12D}$ allosteric site	KRpep-2d	Cyclic – disulphide-linked	Phage display	26
	$KRas^{G12V}$-effector interactions	Compound 12	Cyclic – covalent, Rapalog	Synthetic cyclic library	30
	$KRas^{G12V}$-effector interactions	Cyclorasin 9A5	Cyclic - covalent	Synthetic cyclic library	32
	$KRas^{G12V}$-effector interactions	Peptide 49	Bicyclic – covalently linked	Synthetic bicyclic library	16
	Ras-SOS1 (RasGEF) interaction	HBS3	Hydrogen bond surrogate-stabilised α-helix	SOS1 residues 929-944	34
	KRas-SOS1 (RasGEF) interaction	$SAH\text{-}SOS1_A$	Hydrocarbon-stapled α-helix	SOS1 residues 929-944	36
	Raf dimers	Peptide 38	Cyclic – lactam-bridged	BRaf residues 505-518	40

	Raf dimers	Tat-braftide	Linear, CPP-conjugated	BRaf residues 508-517	41
	RalA/B-effector interactions	SP1	Hydrocarbon-stapled α-helix	RLIP76 (Ral effector) residues 423-446	52
	DiRas3-Beclin1 interaction	Tat-D3S2	Linear, CPP-conjugated	Switch II residues 92-108 of DiRas3	58
Rho	Trio (RhoGEF)	TRIPα	Linear	Yeast two hybrid with aptamers	63
	Tgat (RhoGEF)	TRIPα^{E32G}	Linear	Yeast two hybrid with aptamers	65
	Cdc42-effector interactions	P7	Cyclic – disulphide-linked, CPP-conjugated	CIS display	67
	Rac1-DOCK2 (RacGEF) interaction	DC-pep4	Cyclic – disulphide-linked	Phage display	68
Rab	Rab8a-effector interactions	StRIP14	Double hydrocarbon-stapled α-helix	R6IP (Rab effector) residues 900-916	72
	Rab25-effector complexes	RFP14	Hydrocarbon-stapled α-helix	FIP1 (Rab effector) residues 1245-1274	73
Arf	Arf1 N-terminus mimic	MTM-$Arf1^{2-17}$	Linear, CPP-conjugated	Arf1 residues 2-17	75

2 Ras family

The Ras proteins (HRas, KRas4A, KRas4B and NRas) are known to be the most commonly mutated oncoproteins in human cancer with activating mutations identified in approximately 20% of human tumours and far higher incidences observed in certain cancers e.g. KRas4B in pancreatic (98%) and colorectal (50%) cancers.[24] Oncogenic Ras proteins are typically mutated at positions 12, 13 or 61: these favour the GTP-bound form, rendering Ras constitutively active.[25] As a result of their prevalence in disease, Ras proteins have been the subjects of intense targeting for more than 35 years but despite these efforts there are currently no therapeutics in the clinic that target Ras proteins directly.

2.1 Identification of Ras peptide binders from naïve selections

2.1.1 KRpep-2d

A group at Takeda aimed to identify peptide inhibitors of oncogenic KRas signalling using random libraries in combination with phage display. They screened 10^{11} peptides of varying sizes against the commonly occurring $KRas^{G12D}$ mutant, with phage removed that bound wild-type KRas to enrich for mutant-specific binders.[26] From this selection they identified a disulphide-linked cyclic peptide, KRpep-2 (Figure 2A), with a K_d for $KRas^{G12D}$ of 50 nM, which displayed impressive selectivity over wild-type KRas with 14-fold tighter binding. Addition of a reducing agent drastically decreased binding, demonstrating the importance of the cyclic structure, and a linear control peptide was unable to bind.

The KRpep-2 sequence served as the template for a maturation phage library with the aim of further improving affinity for $KRas^{G12D}$. The most enriched sequence from this library was an identical peptide with two extra Arg residues at the N- and C-termini (KRpep-2d, Figure 2A) that displayed 5-fold improved affinity for $KRas^{G12D}$.[27] This peptide decreased phospho-ERK levels downstream of Ras in a $KRas^{G12D}$ mutant cancer cell line (A427) following dosing at 30 μM but had no effect in a $KRas^{G12C}$ mutant background (A549). The proliferation of the A427 cells was impaired while A549 cells were unaffected, suggesting that this effect was due to KRas mutant-specific inhibition rather than peptide cytotoxicity. The mode of action of KRpep-2d is likely to be due to disruption of GEF-mediated nucleotide exchange, as *in vitro* experiments showed that the peptides could inhibit exchange of GDP for GTP in the presence of the Ras-GEF SOS1, thus preventing activation of $KRas^{G12D}$. The group went on to solve the crystal structure of KRpep-2d in complex with $KRas^{G12D}$·GDP (PDB ID: 5XCO). Interestingly, the peptide binding site is distinct from the SOS1 binding interface and instead KRpep-2d occupies a unique allosteric site on KRas that is adjacent to switch II and the α3 helix (Figure 2B).[27] The peptide appears to form interactions with switch II (Figure 2C), forcing switch II into a conformation that is unfavourable for binding the helical hairpin of SOS1, explaining the observed reduction in SOS1-mediated exchange.

There are, of course, always concerns that disulphide-linked peptides will not remain cyclized in the reducing environment of the cytoplasm and activity will consequently be lost. To circumvent this issue the group investigated several bridging moieties between the two Cys residues of KRpep-2d to produce covalently linked analogues that would be resistant to reduction.[28] Of these, a mono-methylene (-CH_2-) bridge gave rise to the most potent analogue (IC_{50} of 18nM, a modest reduction compared to the IC_{50} of 1.6 nM exhibited by KRpep-2d), which also maintained selectivity for the $KRas^{G12D}$ mutant. This was the shortest linkage tested and was closest to the length of the native disulphide bond. Molecular dynamics simulations indicated that the positions of critical side chains Leu7, Ile9 and Asp12 (identified by Ala-scanning) were maintained with the slightly larger ring size, whereas a much larger bridging molecule, *o*-xylene, greatly affected the overall peptide structure, explaining its much weaker inhibition of $KRas^{G12D}$. *In vitro* assays proved that the methylene-bridged peptide maintained inhibition upon the addition of reducing agent, however unexpectedly the peptide did not display superior performance in cell-based assays, with the stabilized peptide exhibiting similar inhibition to the disulphide-linked KRpep-2d. This suggests that the disulphide linkage in KRpep-2d was maintained inside the cell for long enough for the peptide to exert an effect on Ras signalling, challenging the assumption that a disulphide-linked peptide would be unsuitable for an intracellular target. It is also possible that the introduction of the methylene group reduced cell penetration.

Nevertheless, the high concentrations of these peptides needed for dosing in cell-based assays compared to their *in vitro* affinity suggest that cell entry is poor. Although the peptides only produced minimal effects in cell culture, they could be further developed using new delivery methods including nanoparticles and lipid formulations or by appending a CPP. This is the first example of a peptide that can selectively inhibit a single KRas mutant, providing significant advantages over previous approaches where the lack of specificity over wild-type KRas could lead to significant toxicity issues. This identification of a novel allosteric binding pocket on KRas also offers new options to drug this highly elusive cancer target.

2.1.2 Cyclorasins

The Pei group set out to identify inhibitors of another commonly occurring KRas mutant, G12V, using a synthetic library of cyclic peptides incorporating a rapamycin analogue or 'rapalog', a minimal

motif to recruit FK502-binding protein 12 (FKBP),[29] together with four to six variable amino acid positions for binding to $KRas^{G12V}$.[30] The recruitment of the 12 kDa FKBP protein is used to create a steric block which extends further than the small peptide and therefore could prevent effector binding if oriented correctly.

Peptides selected from the screen that bound to both $KRas^{G12V}$ and FKBP all had the largest ring size tested, containing six variable amino acid positions. Interestingly, many of the peptides were able to inhibit the $KRas^{G12V}$-Raf interaction *in vitro* in the absence of FKBP, indicating that the peptides are bound directly at the effector binding site. The most promising peptide identified, compound 12 (Figure 3A), had a K_d of 0.83 μM for $KRas^{G12V}$ and was able to inhibit a panel of Ras-effector interactions, although no cellular activity was observed due to poor uptake of the peptide.

The apparent lack of cellular uptake for compound 12 was surprising as it contained an Arg-Arg-Nal-Arg-Fpa (Nal = D-β-naphthylalanine, Fpa = L-4-fluorophenylalanine) sequence which closely resembled potent CPPs recently identified by the group.[31] A second synthetic cyclic library to search for intrinsically cell penetrant $KRas^{G12V}$ inhibitors was constructed with the Arg-Arg-Nal-Arg-Fpa core sequence in addition to between one and five randomised positions.[32] One of these hits, Cyclorasin 9A, showed some cell permeability and had a relatively potent IC_{50} of 0.65 μM for the Ras-Raf interaction *in vitro*. This peptide was further optimised based on insights from an Ala scan. The substitution of a Gln for Arg in conjunction with other modifications resulted in a much more cell-permeable peptide, Cyclorasin 9A5 (Figure 3B), which displayed diffuse cytosolic localization and around 4-fold higher affinity for $KRas^{G12V}$. The peptide showed preference for the GTP-bound form of $KRas^{G12V}$ over GDP, indicating that it was binding at or near the switch regions and this was supported by NMR titration experiments. Cyclorasin 9A5 had an anti-proliferative effect on H1299 ($NRas^{Q61K}$ mutant) lung cancer cells and showed a reduction in phosphorylation of targets downstream of Ras (MEK, ERK and Akt) at dosing concentrations above 3 μM. However, the peptide was not able to discriminate between Ras isoforms or between mutant and wild-type KRas, which could lead to future cytotoxicity issues.

2.1.3 Bicyclic Ras inhibitors

The same group also used a synthetic library of bicyclic peptides, 6-10 residues in size, to identify inhibitors of $KRas^{G12V}$.[33] They identified peptides with low micromolar affinity, of which one, Cyclorasin B3, showed preference for KRas·GTP over the GDP-bound form and was competitive with Raf Ras-binding domain (RBD) binding. Monocyclic and linear forms of the peptide had reduced affinities, indicating the benefit of the rigidified structure. The addition of oleic acid to aid cell penetration resulted in a peptide with only modest antiproliferative activity in a lung cancer cell line.

They went on to design a second bicyclic peptide library based on a scaffold in which one of the rings encompassed a cyclic CPP previously identified by the group, $cF\Phi R_4$, where Φ is L-2-napthylalanine,[31] and the second ring contained five positions which could include a variety of proteinogenic and unnatural amino acids to generate target binding affinity.[16] This approach was used to again search for a direct $KRas^{G12V}$ inhibitor. L-propargylglycine (Pra) was included in the peptide sequence and was coupled through click chemistry to 4,6-dichloro-2-methyl-3-aminoethylindole (DCAI), a previously identified KRas small molecule inhibitor with K_d ~ 1 mM that is known to bind proximally to the effector binding region on KRas. This was included with the twin aims of generating peptides that bind close to the effector binding site and improving affinity.

The hit with the best *in vitro* binding affinity (5 μM) was selected for further optimisation and additional Ala residues were added to the ring to determine whether affinity could be improved with

ring expansion. It was found that addition of three Ala residues gave a 5-fold improvement in binding affinity. This larger template formed the basis of a maturation library in which the three Ala residues were replaced with a selection of 25 natural and unnatural amino acids. The second library did not produce a peptide with improved affinity, however it did show that D-Leu and Asp could be included to improve proteolytic stability and solubility. The optimised peptide 49 (Figure 3C) showed a dramatic reduction in binding when the DCAI molecule was removed (0.21 µM vs 17 µM) indicating that the binding site for the DCAI was conserved and indeed competition experiments with free DCAI proved this to be the case. Binding of peptide 49 was shown to be competitive with the Raf RBD but displayed little preference for the nucleotide state of $KRas^{G12V}$, which is surprising given that the conformation of the Raf-binding region changes dramatically depending on whether KRas is bound to GDP or GTP. The binding of the peptide to wild-type KRas or mutants other than G12V was not reported, although general selectivity of the peptides for $KRas^{G12V}$ over unrelated control proteins was demonstrated. Inhibition of signalling downstream of Ras was investigated in two Ras mutant lung cancer cell lines and reduction of p-Akt and p-MEK levels were observed with 18 µM dosing of peptide 49, indicating that the peptide is cell-penetrant and able to reach its target, while a control peptide lacking the DCAI moiety had no effect.

2.2 Inhibition of the Ras-GEF interaction

2.2.1 Hydrogen bond surrogate SOS1 peptides

The first peptides to inhibit Ras based on the Ras-GEF, SOS1, were generated by Patgiri *et al*. who noted that within the helical hairpin region of SOS1, the majority of contacts with KRas are made by one helix, αH (Figure 4A, PDB: 1NVW).[34] Computational models combined with mutagenesis data revealed that Phe929-Asn944 (Figure 4B) were the residues most critical for binding. They designed a peptide based on this sequence and utilised a hydrogen bond surrogate (HBS) approach in which the hydrogen bond between the backbone carbonyl of the N-terminal residue and the amine of the N + 4 residue is replaced with a covalent bond to stabilize a helical conformation.[35] They improved the solubility and helicity of the peptide by replacing non-essential hydrophobic residues with charged residues that have the potential to form stabilizing *i*, *i* + 4 salt bridges. The resulting peptide, HBS3 (Figure 4B), had an affinity of 28 µM for nucleotide free Ras and 158 µM for the GDP-bound state. A titration with ^{15}N labelled Ras and excess peptide to indicate residues involved in peptide binding showed several that were also involved in SOS1 binding. Accordingly, the peptide was able to inhibit SOS1-mediated exchange of GDP for GTP *in vitro*, while a control peptide with key residues mutated to Ala had little effect.

Microscopy showed fluorescent peptide present inside the cell, with punctate staining suggesting that it could be trapped in endosomes. Despite this, an effect on Ras signalling was observed with 75 µM peptide dosing, as shown by a reduction in phospho-Erk levels, suggesting that at least some of the peptide was able to escape into the cytosol and reach its target.

2.2.2 Hydrocarbon stapled SOS1 peptides

Walensky and colleagues also generated peptides based on the helical portion of SOS1 that is involved in KRas binding.[36] They used all-hydrocarbon stapled peptides encompassing the same sequence (SOS1 929-944) with four different *i*, *i* + 4 staple positions. Binding to wild-type KRas and a panel of KRas mutants (G12D/G12V/G12C/G12S/Q61H) was assessed by fluorescence polarisation and three out of four peptides bound all KRas forms with affinities between 60 and 100 nM. The fourth peptide contained a staple position replacing residues that contact KRas in the SOS1 structure, therefore disrupting the normal binding interface, and this peptide showed no binding. Two N-terminal Arg residues were appended to the peptides to alter the overall charge from -1 to

+1, as this has previously been shown to improve cell permeability.[22] The peptide with the best solubility profile was taken forward for further evaluation along with the non-binding control peptide, and these modified peptides were named SAH-SOS1$_A$ (Figure 4B) and SAH-SOS1$_B$ respectively. SAH-SOS1$_A$ was able to disrupt KRas/SOS1 interactions *in vitro* and this was supported by NMR titration data with ^{15}N labelled wild-type KRas and unlabelled peptide, which showed perturbation of several KRas residues implicated in SOS1 binding. The SAH-SOS1$_A$ peptide was able to block intrinsic nucleotide exchange as demonstrated by relative fluorescence using mant-labelled GTP and GDP but it was not reported whether the peptides could also inhibit SOS1-mediated exchange, which would be a requirement for inhibition in a cellular context. The SAH-SOS1$_A$ peptide decreased viability of a variety of cancer cells carrying either wild-type or mutant KRas, while the control peptide SAH-SOS1$_B$ had no effect, demonstrating a sequence-specific effect on the cells tested.

2.3 Targeting a Ras effector: inhibitors of Raf dimerization

Difficulties in targeting Ras directly have led many groups to look for targets downstream of Ras instead, including several proteins in the Raf-MEK-ERK pathway. The Raf isoform BRaf is itself frequently mutated in cancer and these mutations occur independently of activating Ras mutations. Several small molecules targeting the ATP-binding site of BRaf are available in the clinic and can be effective in treating Raf mutant cancers but have proven ineffective in treating Ras mutant cancers, as paradoxical activation of the pathway can occur leading to aggressive tumour recurrence.[37,38] This activation occurs in part due to increased BRaf and CRaf hetero- and homodimer formation,[37,38] therefore inhibition of these dimers offers an opportunity to inhibit oncogenic Raf signalling or increase the potency of existing drugs.

Freeman *et al.* first demonstrated the potential of using peptides to disrupt the Raf dimer interface.[39] By screening several peptides forming segments of the dimer interface they identified residues 503-521 as an effective block of Raf heterodimer formation when expressed in cells: their expression led to decreased phosphorylation of MEK (a substrate of Raf), demonstrating the possibility of targeting this interface for therapeutic intervention.

Beneker *et al.* truncated this peptide at each end and identified 504-518 as a tighter binder than the original sequence (0.13 vs 3.8 μM for 503-521).[40] The shortened peptide 504-518 fused to a Tat CPP showed a reduction in paradoxical MEK activation in cells treated with Vemurafenib, another ATP-competitive BRaf inhibitor. They used available dimer structures to identify possible cyclization points to stabilize the bioactive loop conformation and found several residues in close proximity as possible candidates. They cyclized the shorter peptide (505-518) by lactamization between positions 508 and 513 (Figure 5) and replaced Asn512 with Ala to produce a peptide with a K_d of 61 nM for BRaf, while the linear counterpart had no detectable binding. Unfortunately, no cellular activity of the cyclic peptide was reported.

Another shortened peptide was generated by Gunderwala *et al.* who identified a 10mer encompassing residues 508-517 of BRaf from PeptiDerive predictive software using the crystal structure of BRaf dimers (Figure 5).[41] Their CPP-conjugated peptide, Tat-braftide, acted synergistically with dabrafenib, a Raf ATP-binding site inhibitor, to alleviate the paradoxical activation that is seen with the use of ATP-competitive inhibitors alone. Despite the nanomolar potency reported *in vitro*, very high concentrations of Tat-braftide (75 μM) were required to see an effect in cell culture.

The binding site of these peptides overlaps with the Raf heterodimer interface so the peptides should have the ability to inhibit formation of BRaf homodimers and BRaf/CRaf heterodimers, whose role in resistance to traditional Raf inhibitors has been established.[37,38] These studies demonstrate the tractability of targeting this previously unexplored dimerization interface for the treatment of Ras mutant cancers.

2.4 Targeting Ras multimers

For years there has been conflicting data as to whether Ras functions as a monomer or forms higher order structures but there is now mounting evidence that Ras needs to form dimers or clusters in a cell in order to signal (reviewed in [42]). The α4 and α5 helices, which are distal from the switch regions, have been suggested to drive dimer formation as the vast majority of active Ras crystal structures dimerise via these helices.[43] Inhibition of this interface using a monobody, a small synthetic protein based on a fibronectin type III domain, inhibited oncogenic Ras signalling in cell culture and slowed tumour growth and progression *in vivo* in a nude mouse model bearing KRas mutant tumours.[43,44]

Designed ankyrin repeat proteins (DARPins) have been used to inhibit Ras multimer formation through an interaction involving the α3-α4 helices of KRas, which have also been implicated as a possible interface driving dimer formation.[45,46] Bery *et al.* used phage display with DARPin libraries to identify inhibitors of KRas and an X ray structure of one of their hits revealed that the DARPin interacts with the α3-α4 helices of KRas.[47] The DARPin was able to inhibit mutant KRas dimerization, as well as inhibiting KRas-Raf interactions, leading to a decrease in signalling.

These insights provide a novel opportunity to inhibit Ras signalling through disruption of dimer formation, for which peptides could be utilised in a similar manner to the Raf dimerization inhibitors explored earlier (Section 2.3). This approach could be limited however, as a dimer-targeting tool may not be able to discriminate between wild-type and mutant Ras proteins.

2.5 RalA/B

The Ral-GEF/Ral (Ras like) signalling pathway is activated downstream of active Ras and has been implicated as critical for the survival of several Ras mutant cancers.[48,49] The two Ral proteins, RalA and RalB, are 82% identical and share the same panel of effectors. Despite the high degree of similarity they have divergent roles in tumorigenesis: RalA is required for anchorage-independent growth, while RalB is involved in invasion and metastasis.[50,51]

We used our structure of the RalB/RLIP76 Ral-binding domain (RBD) complex to guide design of peptides to inhibit Ral-effector interactions (Figure 6A).[52] The structure revealed that RLIP76 interacts with RalB through a coiled-coil domain where more than 80% of the contacts with Ral are made through the C-terminal helix of the RLIP76 coiled-coil.[53] This helix was used as a template to generate a series of all-hydrocarbon stapled peptides targeting Ral proteins. Stapling successfully produced peptides with greater helicity and improved target binding compared to the unstapled parent sequence. The tightest-binding peptide (Figure 6B) was selective for active Ral and was shown to be competitive with two Ral effectors, RLIP76 and Sec5. The stapled peptide could penetrate HEK293T cells and inhibited autophagy, a RalB-dependent process, in a GFP-LC3 assay. Work is currently underway in our lab to produce second generation peptides with higher affinity and improved cellular activity.

2.6 DiRas3

In contrast to the tumorigenic Ras proteins, the closely related DiRas (Distinct subgroup of the Ras superfamily) proteins have been identified as tumour suppressors in breast and ovarian cancers as they inhibit growth and metastasis.[54–56] DiRas3, the best-studied member, is downregulated in 60% of breast and ovarian cancers by transcriptional regulation and through silencing by methylation.[57] Another tumour-suppressor role for DiRas3 has recently been identified, through inhibition of Ras multimerization leading to decreased oncogenic Ras signalling.[58] It was found that DiRas3 interacts with the α5 helix of Ras, which has been implicated as part of a potential Ras dimer interface.[43] This finding suggests that peptides mimicking DiRas3 could be used to inhibit Ras multimers.

In contrast to its role as a tumour suppressor in breast and ovarian cancers, DiRas3 has been shown to interact with Beclin1 in the formation of the autophagosome initiation complex.[59,60] Although autophagy can be a suppressor of tumorigenesis, the process has more commonly been shown to facilitate survival of dormant tumour cells in a nutrient-deprived environment and promote tumour survival and aggressiveness.[61] Therefore, inhibitors of autophagy are highly desirable and could be used to increase the effectiveness of existing cancer therapeutics.

As the site of interaction between DiRas3 and Beclin1 was previously unknown, Sutton *et al.* used a peptide array spanning the sequences of DiRas3 and Beclin1 to define the interacting residues. They identified the N-terminal region and switch II of DiRas3 as necessary for the interaction with Beclin1 and went on to generate a peptide based on switch II of DiRas3 (residues 92-108, Figure 7) fused to a Tat CPP (Tat-D3S2). While many small GTPases have highly conserved switch regions, DiRas3 is distinct from other subfamily members in this region and shares only 35% sequence identity with DiRas1 and DiRas2 (Figure 7B) suggesting the potential for peptide specificity in this case.

A K_d value of 1.9 nM between the peptide and Beclin1 was measured by surface plasmon resonance (SPR), although significant binding of the Tat sequence alone and a scrambled peptide control was also observed. Cell entry was confirmed by flow cytometry, and viability of two ovarian cancer cell lines, SKOV3 and A2780, under amino acid starvation conditions was measured using a CellTiter-Glo assay after incubation with 50 μM Tat-D3S2, a scrambled control peptide or Tat alone. Only Tat-D3S2 affected the viability of SKOV3 cells, however for A2780 cells reduced viability was observed for Tat-D3S2 and the scrambled control, indicating off-target effects and toxicity of the sequence. A reduction in autophagy in the SKOV3 cells after Tat-D3S2 treatment was confirmed by a western blot showing reduced LC3-II levels and through quantification of autophagosomes by transmission electron microscopy.

3 Rho family

Several Rho family members play an established role in human cancer. In particular RhoA, Rac1 and Cdc42 have been implicated in the process of metastasis as a consequence of their role in regulation of the actin cytoskeleton.[2] For Rho family members their deregulation most frequently occurs through overexpression of the GTPases and their GEFs or through loss of the negative regulatory GAP proteins, although rarer instances of activating mutations have also been observed.[2,62]

3.1 RhoA

Schmidt *et al.* sought to identify peptides targeting a Rho-GEF, Trio, aimed at targeting the TrioGEFD2 domain that is responsible for activation of RhoA.[63] The TrioGEFD2 domain was used as bait in a yeast two hybrid screen in which a library of 2 x 10^6 aptamers, short peptides fused to a thioredoxin scaffold, were screened. This approach allows *in cellular* screening, which is a more

rigorous test for target specificity, while confining the peptide within a folded protein protects it from proteolytic degradation. Three aptamers taken forward for further testing were found to bind Trio selectively when tested against a panel of related and unrelated proteins, but only TRIAPα (Trio Inhibitory Aptamer), containing a 42 amino acid peptide, was able to inhibit the Rho-GEF function *in vitro* in a GDP release assay. The unscaffolded, linear peptide derived from TRIAPα, termed TRIPα (Trio Inhibitory Peptide), had very similar activity to the aptamer. However, while reducing the length of the peptide in the aptamer to residues 9-36 retained complete activity, truncations in the free peptide form were not tolerated and activity was lost. They went on to test the peptide in cell culture by expressing GFP-tagged TRIPα, which was shown to interact with Trio, causing a reduction in cellular levels of active RhoA.

The group later used this peptide as a template to design peptides targeting Tgat, a Rho-GEF with reported oncogenic potential.[64,65] Tgat is an alternatively spliced form of Trio, consisting of the Trio DH2 domain and a unique C-terminal extension. The original peptide, TRIPα, displayed only very weak affinity for Tgat, as the peptide bound both the DH2 and PH2 domains of Trio. To search for peptides with tighter binding to Tgat, which lacks the PH2 domain, the Trio DH2 domain alone was used as bait in an optimization yeast two hybrid assay, in which TRIPα aptamers were subjected to random mutagenesis. Tgat itself could not be used as bait as it is toxic when expressed in yeast. They found that a single E32G mutant improved the affinity of the peptide for Tgat from 90 to 7 μM and improved the Tgat GEF inhibition 15-fold. The mutated peptide had equivalent efficacy against Trio and Tgat but was selective over other Rho-GEFs and Rho family members tested. The peptide reduced RhoA activation levels in Tgat-expressing NIH3T3 cells and was able to inhibit Tgat-mediated transformation of the cells when co-expressed as a GFP fusion. Nude mice injected with NIH3T3 cells co-expressing Tgat and GFP-TRIPα^{E32G} peptide had a dramatically reduced tumour onset and volume compared to those expressing Tgat in the absence of the peptide.

These studies provide strong validation of Rho-GEFs as therapeutic targets and demonstrate the benefit of inhibiting the RhoA/GEF interaction, although converting these large, linear peptides to proteolytically stable and cell-penetrant therapeutic candidates could prove challenging.

3.2 Cdc42

Cdc42 is another small GTPase that is upregulated in several cancer types.[2] Work carried out in our lab aimed to develop a peptide inhibitor of Cdc42/effector interactions using naïve libraries of short linear (10/12mer), long linear (16/20/25mer) and cyclic sequences (14-18mer) with Cys residues at N + 4 and C - 4 positions. CIS display[66] was used to screen the libraries of peptides against active Cdc42 and competitive binders were identified by elution with the G protein binding domain of ACK, an effector for Cdc42.[67]

This approach identified several enriched sequences of which one, a 16mer termed C1 identified from the cyclic library, displayed a K_d of 350 nM for Cdc42 and was competitive with the Cdc42 effector, ACK. The binding was dependent on the cyclic structure of the peptide and addition of reducing agent or mutation of the Cys residues to Ser, disabling disulphide bond formation, ablated binding to Cdc42.

The cyclic C1 peptide was matured in a second CIS display selection in which the positions with lowest amino acid consensus were allowed to alter. Several sequences were identified with significantly higher affinity for Cdc42, giving 5 to 20-fold improvement compared to the parent (C1) sequence. An NMR titration with ^{15}N-labelled Cdc42 and the matured peptide P7 demonstrated that the peptide binding site overlaps with known binding sites of multiple Cdc42 effectors.

Upon addition of a nona-arginine cell-penetrating motif, P7 was able to enter cells and was used for phenotypic studies. The peptide inhibited proliferation and migration of a lung cancer cell line and was shown to interact directly with Cdc42 in cells by cellular thermal shift assays (CETSAs), unusually resulting in a destabilization of Cdc42 in the presence of P7.

3.3 Rac1

A group at Takeda used random library screening with T7 phage to search for inhibitors of the interaction between Rac1 and its GEF, DOCK2.[68] In the selection, peptides that bound to DOCK2 were eluted with Rac1 to select for competitive binding. A disulphide-containing cyclic peptide, DC-pep4, with a low nanomolar IC_{50} value was shown to be selective for DOCK2 over the highly similar DOCK1 protein and was able to inhibit DOCK2-mediated exchange of GDP for GTP on Rac1. Interestingly, the peptide still exhibited tight binding, albeit with 10-fold lower affinity, in reducing conditions (K_d of 1.8 nM vs 0.17 nM in non-reducing conditions) in contrast with the previous examples of the cyclic KRas-binding peptide KRpep-2d and our Cdc42-binding peptides where maintenance of the disulphide was critical for the binding activity of the peptide.[26,67]

The peptide was further optimised by truncation of the three N-terminal residues and by addition of *o*-xylene to covalently link the cysteine residues. Several other linkers were tested but resulted in a loss of affinity as the ring size increased. DC-pep4 already contained three Arg residues at the C-terminus and an additional five Arg residues were added across the N- and C-termini to promote cell penetration.

Cytosolic entry of the peptides was investigated by a novel method involving the conjugation of luciferin via a disulphide linkage to the peptide. Upon entry to the reducing environment of the cytosol, the luciferase substrate is released and produces a luminescent signal in cells transfected with luciferase. The peptide containing eight terminal arginines was shown to effectively penetrate the cytosol and induced inhibition of migration in a human B lymphocyte cell line (MINO) with an IC_{50} of approximately 120 nM. The group set out to improve cytosolic entry further by assessing the uptake of 13 known CPPs in addition to novel CPPs based on a viral protein from influenza A using their luciferin assay.[69] They found that their novel CPP, termed PF5, and an octa-Arg motif both resulted in peptides with dramatically improved cellular uptake and a concordant improvement in inhibition of cell migration.

4 Rab family

The Rab proteins are deregulated in a broad range of human diseases including cancer, diabetes, neurodegenerative diseases and infectious diseases.[5,70] This deregulation occurs due to overexpression of the GTPases or through upregulation via altered expression of their regulatory proteins.

4.1 Rab8a

Spiegel *et al*. set out to develop inhibitors of Rab-effector interactions and searched for Rab effectors that interact via α-helical motifs and bury an extensive surface area on binding, to act as templates for stapled peptide design. Multiple Rab effectors: R6IP, LidA, REP1 and Rabin8, were found to bind Rab proteins via an α-helix and a series of peptides based on these interacting helices was generated.[71] Hydrocarbon stapling was effective at improving binding affinity, with increases of up to 200-fold compared to the linear precursors. Binding was observed for a range of Rab family members, and most peptides tested bound the nucleotide-free forms more tightly than the GDP or GTP-bound proteins. It was hypothesised that this is due to the possibility of an induced fit upon

binding as a result of increased flexibility in the nucleotide-free structure. Promisingly, the stapled peptide StRIP3 (based on R6IP, Figure 8A and B) bound Rab8a·GTP with an affinity of ~20 μM and was able to compete for the Rab8a/OCRL1 effector interaction. This peptide was optimised further to improve affinity, cell uptake and proteolytic stability.[72] The incorporation of a second staple slightly improved the affinity for Rab8a and the resulting peptide, StRIP14 (Figure 8B), displayed a K_d of 7.8 μM and bound Rab8a more than 10-fold tighter than related Rab family members. This double-stapled peptide had dramatically improved proteolytic stability, from the StRIP3 $t_{1/2}$ of 0.30 min to more than 95% of the peptide remaining after 48 hours in a proteinase K degradation assay. Cell permeability was achieved by the replacement of negatively charged residues (Asp, Glu) with their neutral analogues (Asn, Gln) after an arginine scan showed that substitutions with Arg residues were not well tolerated. The resultant peptide was able to enter cells with a similar efficiency to the CPP Tat_{49-57} sequence and displayed endomembrane localization that overlapped with that of Rab8a.

4.2 Rab25

Peptides for Rab25 have also been generated based on the Rab11 family of interacting proteins, the FIPs, which bind Rab11/25 proteins using an α-helix followed by a turn and a short 3_{10} helix (Figure 8C).[73] Stapled peptides based on the Rab binding domains of FIP1-4 were generated, leading to the identification of stapled peptides which bound with sub-micromolar affinity and displayed preference for Rab25 over Rab11a. Cellular penetration was improved by the replacement of anionic residues with neutral polar or cationic residues and with the addition of extra charge at the peptide terminus. The optimised peptide RFP14 (Figure 8D) was able to effectively enter HEY cells (an ovarian cancer cell line) and reversed the global expression profile associated with Rab25 overexpression.

5 Arf family

The small GTPase Arf1 has been implicated in allergic responses and inflammation: Nishida *et al.* demonstrated that Arf1 activation results in mast cell degranulation and set out to develop inhibitors of this activation as a potential treatment for inflammation.[74]

The group generated peptides based on the N-terminal region of Arf1 fused to a CPP called MTM.[75] Having previously identified that MTM-Arf1 (residues 2-17) inhibited mass cell degranulation,[74] they aimed to find the minimal binding sequence required for such an effect. Truncation from the C-terminus showed that Lys15 and Lys16 were essential for the activity of the peptide, while Glu17 could be lost with no significant effect on activity. At the N-terminus, removal of amino acids up to Lys10 did not dramatically effect activity but Lys10 itself was shown to be essential. The shortened peptide MTM-Arf1(8-16) inhibited cytokine production and caused a decreased allergic response in a mouse model of anaphylaxis. Unfortunately, no studies were carried out to elucidate the mechanism of action of the peptide, although it was proposed that the peptide can block Arf1 localization at the membrane, which is essential for its function.[76] Arf1 requires myristoylation at its N-terminus for membrane localization and the peptide lacks the N-terminal Gly residue that is normally modified and so cannot be exerting its effect through inhibition of the myristoylation event. Instead, the authors hypothesized that the three essential lysine residues in the peptide play a critical role in its mode of action by inhibiting the interaction of Arf1 with membrane phospholipids, particularly PIP_2. The N-terminal region of Arf1 explored in this study forms a helix, so a peptide based on this region could benefit from helix stabilization chemistries to protect the peptide from proteolytic degradation and potentially improve cell penetration without the use of a CPP.

6 Future directions

The examples discussed in this review clearly show that peptides with high affinity and selectivity can be generated for a wide range of targets. The *in vivo* activity of these peptides, however, is often limited by poor and unpredictable cell penetration properties. Examination of cell-permeable macrocycles from nature has provided valuable insights into peptide design, including N-methylation of backbone residues which has helped to improve permeability of synthetic peptides.[14,15] The advent of peptide stapling and subsequent studies into the cell-penetrating properties of such peptides have provided a set of design principles for targeting intracellular targets mediated via α-helices, improving the chances of producing successful compounds.[22,23,77] While there is still no universal strategy for generating cell-permeable peptides, our understanding of the properties determining cell penetration will only continue to increase and with that will come a dramatic rise in the effectiveness of peptides for intracellular targets. It is unlikely that a single approach can be applied to all of the small GTPases, however with so many avenues being explored to disrupt their function including the use of peptides, covalent inhibitors, DARPins and monobodies, it is only a matter of time before effective therapeutics reach the clinic and serve as inspiration for targeting other members of this highly important family of proteins.

Acknowledgements

Work in our laboratory, discussed in this review, has been supported by grants from the Cambridge Cancer Centre, the MRC (MR/K017101/1), the BBSRC (BB/M011194/1) and the Glover Research Fund. CH is supported by an AstraZeneca/Department of Biochemistry, University of Cambridge Studentship.

Conflicts of interest

The authors have no conflicts of interest to declare.

References

1. K. Wennerberg, J. Cell Sci. **2005**, *118*, 843.
2. R.B. Haga, A.J. Ridley, Small GTPases **2016**, *7*, 207.
3. G.A. Hobbs, C.J. Der, K.L. Rossman, J. Cell Sci. **2016**, *129*, 1287.
4. A. Flentje, R. Kalsi, T.S. Monahan, Int. J. Mol. Sci. **2019**, *20*, 1.
5. A. Prashar, L. Schnettger, E.M. Bernard, M.G. Gutierrez, Front. Cell. Infect. Microbiol. **2017**, *7*, 1.
6. K. Kato, A.D. Cox, M.M. Hisaka, S.M. Graham, J.E. Buss, C.J. Der, Proc. Natl. Acad. Sci. U. S. A. **1992**, *89*, 6403.
7. D.B. Whyte, P. Kirschmeier, T.N. Hockenberry, I. Nunez-Oliva, L. James, J.J. Catino, W.R. Bishop, J. Pai, J. Biol. Chem. **1997**, *272*, 14459.
8. C.J. Novotny, G.L. Hamilton, F. McCormick, K.M. Shokat, ACS Chem. Biol. **2017**, *12*, 1956.
9. A. Ho, N. Chau, I.B. Garcia, C. Ferte, C. Even, F. Burrows, L. Kessler, V. Mishra, K. Magnuson, C. Scholz, A. Gualberto, Int. J. Radiat. Oncol. **2018**, *100*, 1367.
10. A.L. Ho, N. Chau, J. Bauman, K. Bible, A. Chintakuntlawar, M.E. Cabanillas, D.J. Wong, I. Braña Garcia, M.S. Brose, V. Boni, C. Even, M. Razaq, V. Mishra, K. Bracken, D. Wages, C. Scholz, A. Gualberto, Ann. Oncol. **2018**, *29*, 373.
11. J.M. Ostrem, U. Peters, M.L. Sos, J.A. Wells, K.M. Shokat, Nature **2013**, *503*, 548.
12. Z. Qian, P.G. Dougherty, D. Pei, Curr. Opin. Chem. Biol. **2017**, *38*, 80.
13. P. Matsson, B.C. Doak, B. Over, J. Kihlberg, Adv. Drug Deliv. Rev. **2016**, *101*, 42.
14. J. Chatterjee, C. Gilon, A. Hoffman, H. Kessler, Acc. Chem. Res. **2008**, *41*, 1331.
15. J. Chatterjee, F. Rechenmacher, H. Kessler, Angew. Chemie - Int. Ed. **2013**, *52*, 254.
16. T.B. Trinh, P. Upadhyaya, Z. Qian, D. Pei, ACS Comb. Sci. **2016**, *18*, 75.
17. B.N. Bullock, A.L. Jochim, P.S. Arora, J. Am. Chem. Soc. **2011**, *133*, 14220.
18. Y.-W. Kim, T.N. Grossmann, G.L. Verdine, Nat. Protoc. **2011**, *6*, 761.

19. Y.H. Lau, P. De Andrade, Y. Wu, D.R. Spring, Chem. Soc. Rev. **2015**, *44*, 91.

20. D.P. Fairlie, A. Dantas de Araujo, Biopolymers **2016**, *106*, 843.

21. S. Baek, P.S. Kutchukian, G.L. Verdine, R. Huber, T.A. Holak, K.W. Lee, G.M. Popowicz, J. Am. Chem. Soc. **2012**, *134*, 103.

22. L.D. Walensky, G.H. Bird, J. Med. Chem. **2014**, *57*, 6275.

23. G.H. Bird, E. Mazzola, K. Opoku-nsiah, M.A. Lammert, M. Godes, D.S. Neuberg, L.D. Walensky, Nat. Chem. Biol. **2016**, 1.

24. A.D. Cox, S.W. Fesik, A.C. Kimmelman, J. Luo, C.J. Der, Nat. Publ. Gr. **2014**, *13*, 828.

25. I.A. Prior, P.D. Lewis, C. Mattos, Cancer Res. **2012**, *72*, 2457.

26. K. Sakamoto, Y. Kamada, T. Sameshima, M. Yaguchi, A. Niida, S. Sasaki, M. Miwa, S. Ohkubo, J. Sakamoto, M. Kamaura, N. Cho, A. Tani, Biochem. Biophys. Res. Commun. **2017**, *484*, 605.

27. S. Sogabe, Y. Kamada, M. Miwa, A. Niida, T. Sameshima, M. Kamaura, K. Yonemori, S. Sasaki, J. Sakamoto, K. Sakamoto, ACS Med. Chem. Lett. **2017**, *8*, 732.

28. A. Niida, S. Sasaki, K. Yonemori, T. Sameshima, M. Yaguchi, T. Asami, K. Sakamoto, M. Kamaura, Bioorganic Med. Chem. Lett. **2017**, *27*, 2757.

29. X. Wu, L. Wang, Y. Han, N. Regan, P.K. Li, M.A. Villalona, X. Hu, R. Briesewitz, D. Pei, ACS Comb. Sci. **2011**, *13*, 486.

30. X. Wu, P. Upadhyaya, M.A. Villalona-Calero, R. Briesewitz, D. Pei, Medchemcomm **2013**, *4*, 378.

31. Z. Qian, T. Liu, Y.Y. Liu, R. Briesewitz, A.M. Barrios, S.M. Jhiang, D. Pei, ACS Chem. Biol. **2013**, *8*, 423.

32. P. Upadhyaya, Z. Qian, N.G. Selner, S.R. Clippinger, Z. Wu, R. Briesewitz, D. Pei, Angew. Chemie - Int. Ed. **2015**, *54*, 7602.

33. P. Upadhyaya, Z. Qian, N. Habir, D. Pei, Tetrahedron **2014**, *70*, 7714.

34. A. Patgiri, K.K. Yadav, P.S. Arora, D. Bar-Sagi, Nat. Chem. Biol. **2011**, *7*, 585.

35. A. Patgiri, A.L. Jochim, P.S. Arora, Acc. Chem. Res. **2008**, *41*, 1289.

36. E.S. Leshchiner, A. Parkhitko, G.H. Bird, J. Luccarelli, J.A. Bellairs, S. Escudero, K. Opoku-Nsiah, M. Godes, N. Perrimon, L.D. Walensky, Proc. Natl. Acad. Sci. U. S. A. **2015**, *112*, 1761.

37. P.I. Poulikakos, C. Zhang, G. Bollag, K.M. Shokat, N. Rosen, Nature **2010**, *464*, 427.

38. G. Hatzivassiliou, K. Song, I. Yen, B.J. Brandhuber, D.J. Anderson, R. Alvarado, M.J.C. Ludlam, D. Stokoe, S.L. Gloor, G. Vigers, T. Morales, I. Aliagas, B. Liu, S. Sideris, K.P. Hoeflich, B.S. Jaiswal, S. Seshagiri, H. Koeppen, M. Belvin, L.S. Friedman, S. Malek, Nature **2010**, *464*, 431.

39. A.K. Freeman, D.A. Ritt, D.K. Morrison, Mol. Cell **2013**, *49*, 751.

40. C.M. Beneker, M. Rovoli, G. Kontopidis, M. Röring, S. Galda, S. Braun, T. Brummer, C. McInnes, J. Med. Chem. **2019**, *62*, 3886.

41. A.Y. Gunderwala, A.A. Nimbvikar, N.J. Cope, Z. Li, Z. Wang, ACS Chem. Biol. **2019**, *14*, 1471.

42. M. Chen, A. Peters, T. Huang, X. Nan, Rev. Med. Chem. **2016**, *16*, 391.

43. R. Spencer-Smith, A. Koide, Y. Zhou, R.R. Eguchi, F. Sha, P. Gajwani, D. Santana, A. Gupta, M. Jacobs, E. Herrero-Garcia, J. Cobbert, H. Lavoie, M. Smith, T. Rajakulendran, E. Dowdell, M.N. Okur, I. Dementieva, F. Sicheri, M. Therrien, J.F. Hancock, M. Ikura, S. Koide, J.P. O'Bryan, Nat. Chem. Biol. **2017**, *13*, 62.

44. I. Khan, R. Spencer-Smith, J.P. O'Bryan, Oncogene **2019**, *38*, 2984.

45. S. Sarkar-Banerjee, A. Sayyed-Ahmad, P. Prakash, K.J. Cho, M.N. Waxham, J.F. Hancock, A.A. Gorfe, J. Am. Chem. Soc. **2017**, *139*, 13466.

46. P. Prakash, A. Sayyed-Ahmad, K.J. Cho, D.M. Dolino, W. Chen, H. Li, B.J. Grant, J.F. Hancock, A.A. Gorfe, Sci. Rep. **2017**, *7*, 1.

47. N. Bery, S. Legg, J. Debreczeni, J. Breed, K. Embrey, C. Stubbs, P. Kolasinska-Zwierz, N. Barrett, R. Marwood, J. Watson, J. Tart, R. Overman, A. Miller, C. Phillips, R. Minter, T.H. Rabbitts, Nat. Commun. **2019**, *10*, 0.

48. B.O. Bodemann, M.A. White, Nat. Rev. Cancer **2008**, *8*, 133.

49. N.M. Hamad, J.H. Elconin, A.E. Karnoub, W. Bai, J.N. Rich, R.T. Abraham, C.J. Der, C.M. Counter, Genes Dev. **2002**, *16*, 2045.

50. K. Lim, K.O. Hayer, S.J. Adam, S.D. Kendall, P.M. Campbell, C.J. Der, C.M. Counter, N. Carolina, C. Hill, N. Carolina, Curr. Biol. **2006**, *16*, 2385.

51. K. Lim, A.T. Baines, J.J. Fiordalisi, M. Shipitsin, L.A. Feig, A.D. Cox, C.J. Der, C.M. Counter, Cancer Cell **2005**, *7*, 533.

52. J.C. Thomas, J.M. Cooper, N.S. Clayton, C. Wang, M.A. White, C. Abell, D. Owen, H.R. Mott, J. Biol. Chem. **2016**, *291*, 18310.

53. R.B. Fenwick, L.J. Campbell, K. Rajasekar, S. Prasannan, D. Nietlispach, J. Camonis, D. Owen, H.R. Mott, Structure **2010**, *18*, 985.

54. M.N. Sutton, H. Yang, G.Y. Huang, C. Fu, M. Pontikos, Y. Wang, W. Mao, L. Pang, M. Yang, J. Liu, J. Parker-Thornburg, Z. Lu, R.C. Bast, Autophagy **2018**, *14*, 637.

55. D.B. Badgwell, Z. Lu, K. Le, F. Gao, M. Yang, G.K. Suh, J.J. Bao, P. Das, M. Andreeff, W. Chen, Y. Yu, A.A. Ahmed, W. S-L Liao, R.C. Bast, Oncogene **2012**, *31*, 68.

56. Y. Yu, F. Xu, H. Peng, X. Fang, S. Zhao, Y. Li, B. Cuevas, W.L. Kuo, J.W. Gray, M. Siciliano, G.B. Mills, R.C. Bast Jr, Proc. Natl. Acad. Sci. U. S. A. **1999**, *96*, 214.

57. Y. Yu, R. Luo, Z. Lu, W. Wei Feng, D. Badgwell, J.P. Issa, D.G. Rosen, J. Liu, R.C. Bast, Methods Enzymol. **2006**, *407*, 455.

58. M.N. Sutton, Z. Lu, Y.C. Li, Y. Zhou, T. Huang, A.S. Reger, A.M. Hurwitz, T. Palzkill, C.

Logsdon, X. Liang, J.W. Gray, X. Nan, J. Hancock, G.M. Wahl, R.C. Bast, Cell Rep. **2019**, *29*, 3448.

59. M.N. Sutton, G.Y. Huang, X. Liang, R. Sharma, A.S. Reger, W. Mao, L. Pang, P.J. Rask, K. Lee, J.P. Gray, A.M. Hurwitz, T. Palzkill, S.W. Millward, C. Kim, Z. Lu, R.C. Bast, Cancers (Basel). **2019**, *11*, 1.

60. Z. Lu, M.T. Baquero, H. Yang, M. Yang, A.S. Reger, C. Kim, D.A. Levine, C.H. Clarke, W.S.L. Liao, R.C. Bast, Autophagy **2014**, *10*, 1071.

61. E. White, J. Clin. Invest. **2015**, *125*, 42.

62. A.P. Porter, A. Papaioannou, A. Malliri, Small GTPases **2016**, *7*, 123.

63. E. Fabbrizio, A. Debant, S. Schmidt, S. Diriong, J. Me, FEBS Lett. **2002**, *523*, 35.

64. N. Yoshizuka, R. Moriuchi, T. Mori, K. Yamada, S. Hasegawa, T. Maeda, T. Shimada, Y. Yamada, S. Kamihira, M. Tomonaga, S. Katamine, J. Biol. Chem. **2004**, *279*, 43998.

65. N. Bouquier, S. Fromont, J.C. Zeeh, C. Auziol, P. Larrousse, B. Robert, M. Zeghouf, J. Cherfils, A. Debant, S. Schmidt, Chem. Biol. **2009**, *16*, 391.

66. R. Odegrip, D. Coomber, B. Eldridge, R. Hederer, P.A. Kuhlman, C. Ullman, K. FitzGerald, D. McGregor, Proc. Natl. Acad. Sci. **2004**, *101*, 2806.

67. G.J.N. Tetley, N.P. Murphy, S. Bonetto, G. Ivanova-Berndt, J. Revell, H.R. Mott, R.N. Cooley, D. Owen, J. Biol. Chem. **2020**, *295*, 2866.

68. K. Sakamoto, Y. Adachi, Y. Komoike, Y. Kamada, R. Koyama, Y. Fukuda, A. Kadotani, T. Asami, J. ichi Sakamoto, Biochem. Biophys. Res. Commun. **2017**, *483*, 183.

69. Y. Adachi, K. Sakamoto, T. Umemoto, Y. Fukuda, A. Tani, T. Asami, Bioorganic Med. Chem. **2017**, *25*, 2148.

70. J.O. Agola, P.A. Jim, H.H. Ward, S. Basuray, A. Wandinger-Ness, Clin. Genet. **2011**, *80*, 305.

71. J. Spiegel, P.M. Cromm, A. Itzen, R.S. Goody, T.N. Grossmann, H. Waldmann, Angew. Chemie - Int. Ed. **2014**, *53*, 2498.

72. P.M. Cromm, J. Spiegel, P. Küchler, L. Dietrich, J. Kriegesmann, M. Wendt, R.S. Goody, H. Waldmann, T.N. Grossmann, ACS Chem. Biol. **2016**, *11*, 2375.

73. S. Mitra, J.E. Montgomery, M.J. Kolar, G. Li, K.J. Jeong, B. Peng, G.L. Verdine, G.B. Mills, R.E. Moellering, Nat. Commun. **2017**, *8*, 1.

74. K. Nishida, S. Yamasaki, A. Hasegawa, A. Iwamatsu, H. Koseki, T. Hirano, J. Immunol. **2011**, *187*, 932.

75. R. Uchida, T. Egawa, Y. Fujita, K. Furuta, H. Taguchi, S. Tanaka, K. Nishida, Mol. Immunol. **2019**, *105*, 32.

76. J.G. Donaldson, C.L. Jackson, Nat. Rev. Mol. Cell Biol. **2011**, *12*, 362.

77. Q. Chu, R.E. Moellering, G.J. Hilinski, Y. Kim, T.N. Grossmann, T. Yeh, G.L. Verdine, Medchemcomm **2014**, *6*, 111.

Abbreviations

CETSA	Cellular thermal shift assay
CPP	Cell-penetrating peptide
DARPin	Designed ankyrin repeat protein
FTI	Farnesyltransferase inhibitor
GAP	GTPase activating protein
GDI	Guanine nucleotide dissociation inhibitor
GDP	Guanosine diphosphate
GEF	Guanine nucleotide exchange factor
GFP	Green fluorescent protein
GGTase	Geranylgeranyltransferase
GTP	Guanosine triphosphate
PDB	Protein Data Bank
PPI	Protein-protein interaction
RBD	Ras/Ral-binding domain
SPR	Surface plasmon resonance

Figure legends

Figure 1. The Ras superfamily of small GTPases. A. Selected members of the human Ras superfamily. Proteins that have been targeted by peptides and are covered in this review are highlighted in red. B. The GTPase cycle. GTPases are inactive when bound to GDP. Ras, Rho and Rab proteins have associated GDIs and GDI-like partners that can extract them from the membrane in this form, sequestering them in the cytosol. Binding of a GEF causes exchange of GDP for GTP by promoting the loss of GDP followed by GTP binding, which occurs as a result of far higher intracellular concentrations of GTP. In the GTP-bound form the small GTPases are activated and are competent in effector binding. They are then deactivated by binding to GAPs, which stimulate hydrolysis of GTP to GDP. The vast majority of small GTPases are lipid modified and are membrane bound.

Figure 2. Cyclic peptide KRpep-2d binding to KRas. A. Sequences of KRpep-2 and KRpep-2d. Cys residues that cyclize the peptide are highlighted in red. B. Crystal structure of KRpep-2d bound to $KRas^{G12D}$·GDP (PDB ID: 5XCO). KRas is shown in blue, with switch I (yellow) and switch II (green) highlighted. GDP nucleotide is shown as sticks. The peptide (orange) binds at a site proximal to switch II and the α3 helix. C. Zoom of the structure with contacts formed between KRpep-2d and KRas shown as dashed lines, including a hydrogen bond between the backbone NH of KRpep-2d Tyr8 and the backbone carbonyl of Gln61 on KRas (indicated by *).

Figure 3. Macrocyclic Ras inhibitors. A. Compound 12 identified from a screen of cyclic peptides incorporating a FKBP binding motif (red). Amino acid positions varied in the screen are labelled 1-6. B. Structure of Cyclorasin 9A5, a cyclic peptide identified from a library of peptides containing a CPP sequence identified previously (blue) and up to 5 variable amino acid positions (labelled 1-5). C. Structure of an optimised hit from a bicyclic library screen, peptide 49. DCAI = 4,6- dichloro-2-methyl-3-aminoethylindole, a KRas inhibitor (green).

Figure 4. Helical peptides targeting the Ras-SOS1 interaction. A. Crystal structure of nucleotide free HRas (blue; switch I, yellow; switch II, green) in complex with SOS1 (grey, PDB ID: 1NVW). Residues 929-944 of SOS1 are coloured in orange. B. Peptides generated based on SOS1. X = (*S*)-pentenylalanine, Z = 4-pentenoic acid. Substitutions from the parent sequence are shown in red.

Figure 5. Inhibition of Raf dimerization. A. Crystal structure of active Raf dimers (PDB: 4E26). One monomer is displayed in blue and the other in grey with residues 504-518 coloured in orange. Zoom shows the position of residues 508 and 513 as sticks that were used for lactamization by Beneker *et al.*[38] B. Peptides designed to inhibit BRaf dimer formation. Residues altered from the original Raf sequence are shown in red. The cyclic peptide has undergone lactamization at Lys4 (BRaf numbering 508) and Glu9 (BRaf 513).

Figure 6. Inhibition of Ral GTPases. A. NMR structure of RalB·GMPPNP (blue; switch I, yellow; switch II, green) in complex with the RLIP76 RBD (grey, residues 423-446 in orange, PDB ID:2KWI). GMPPNP is shown as sticks and the Mg^{2+} cation is displayed as a yellow sphere. B. The sequence of the tightest binding peptide identified based on the RLIP76 RBD is shown. X = (*S*)-pentenylalanine.

Figure 7. Inhibition of DiRas3. A. Crystal structure of DiRas2 (blue; Switch I, yellow; PDB ID:2ERX) with switch II residues that form the basis for the DiRas3-derived peptide shown in orange. GDP is shown as sticks and the Mg^{2+} cation is represented by a yellow sphere. B. A sequence alignment of switch II from the three DiRas isoforms shows large disparity between DiRas3 compared with DiRas1 and 2. Identical and similar residues are coloured orange; divergent residues are coloured black.

Figure 8. Helical effectors for Rab proteins as the basis for peptide inhibitors. A. Crystal structure of Rab6·GTP (blue; switch I, yellow; switch II, green) in complex with R6IP (grey; residues 900-916, orange; PDB ID: 3CWZ). The nucleotide is shown as sticks and the Mg^{2+} cation is represented by a yellow sphere. B. Peptide sequences derived from residues 900-916 of R6IP. C. Crystal structure of Rab25·GMPPNP (blue) in a symmetrical dimer complex with FIP2 (grey; residues 471-500, orange; PDB ID: 3TSO). The region of FIP2 highlighted in orange is equivalent to residues 1245-1274 in FIP1. D. Sequence of peptide RFP14 derived from FIP1 (1245-1274). Residues that have been modified from the original sequence are highlighted in red. X = (*S*)-pentenylalanine, N_L = norleucine, β = beta-alanine.

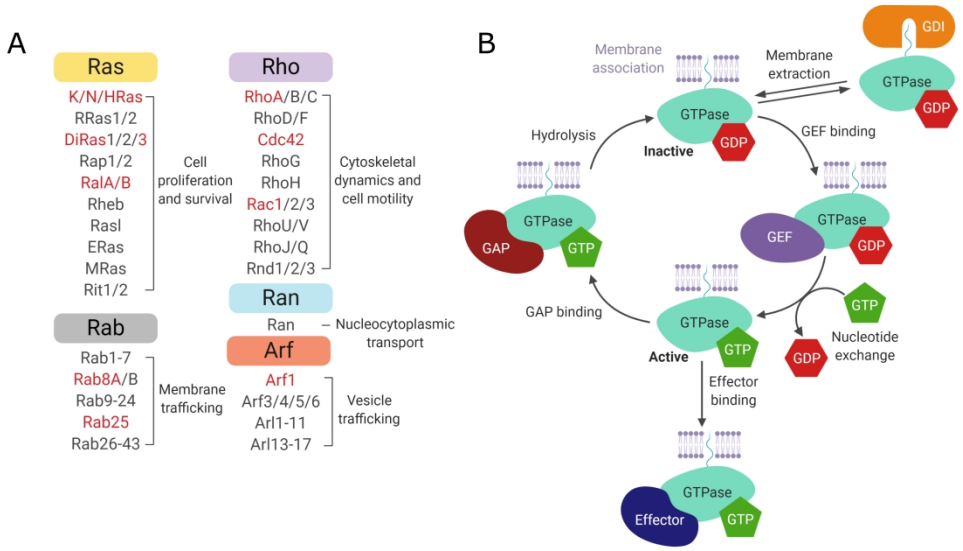

Figure 1

398x230mm (300 x 300 DPI)

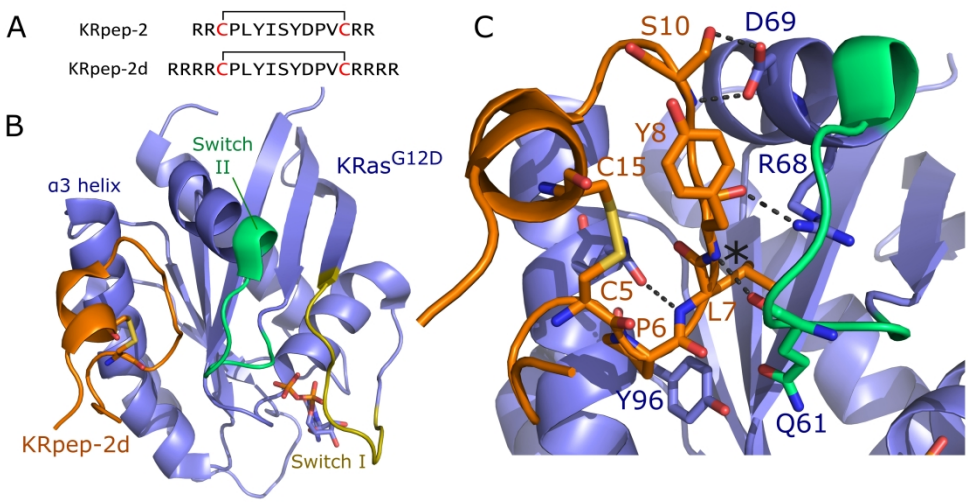

Figure 2

383x198mm (300 x 300 DPI)

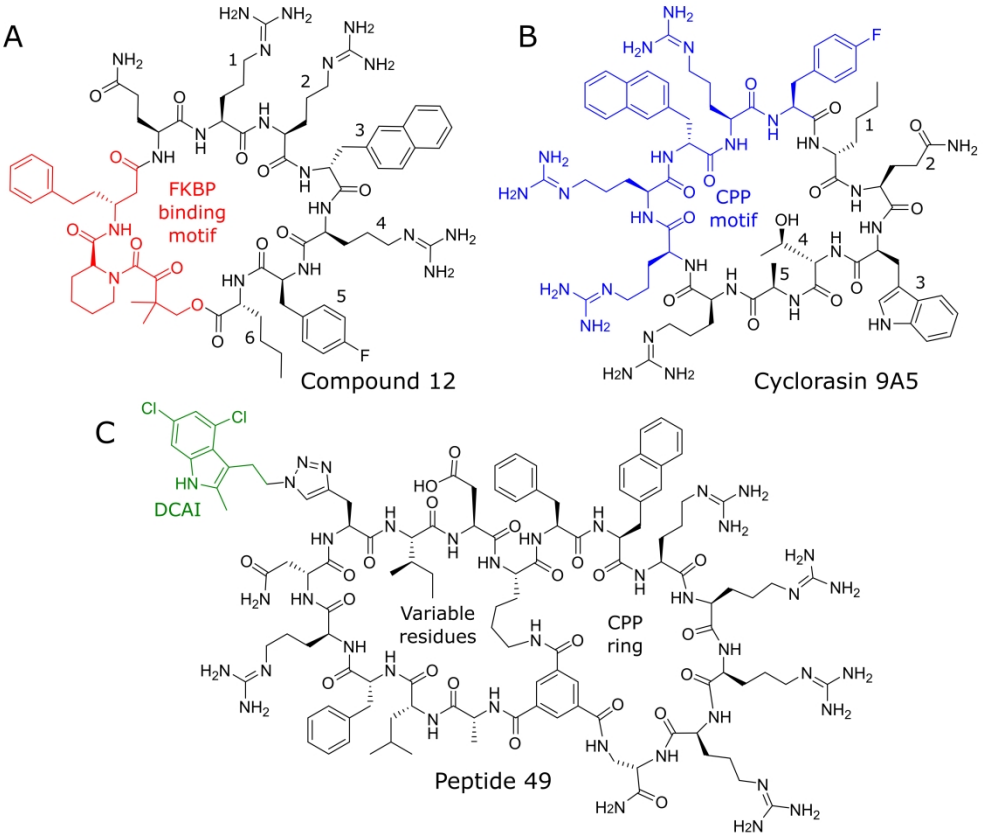

Figure 3

381x326mm (300 x 300 DPI)

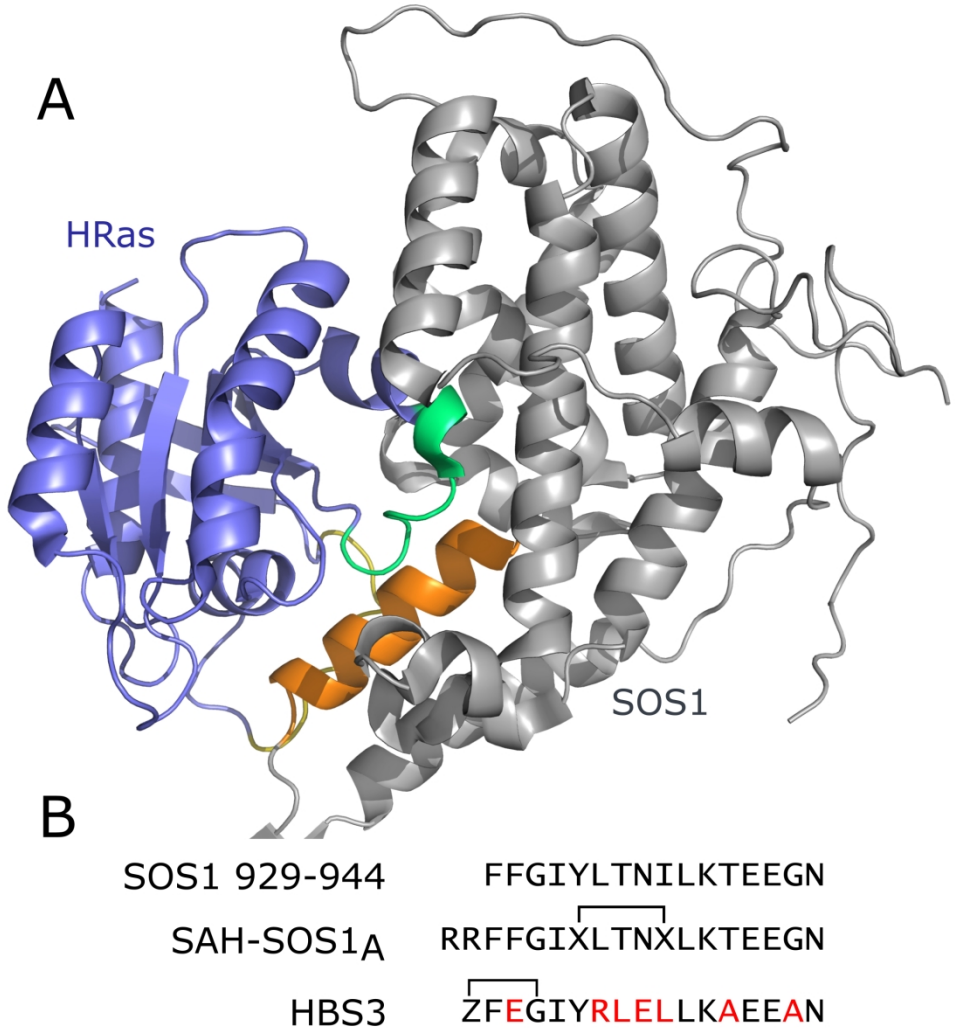

Figure 4

198x210mm (300 x 300 DPI)

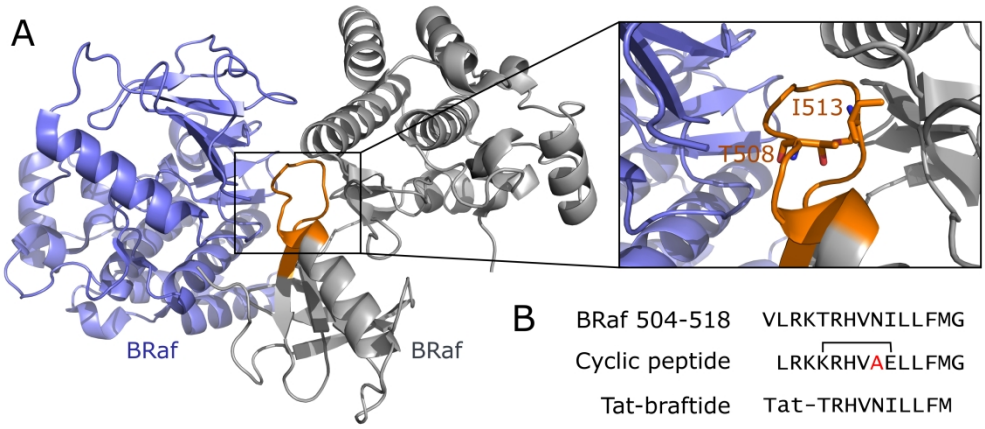

Figure 5

315x141mm (300 x 300 DPI)

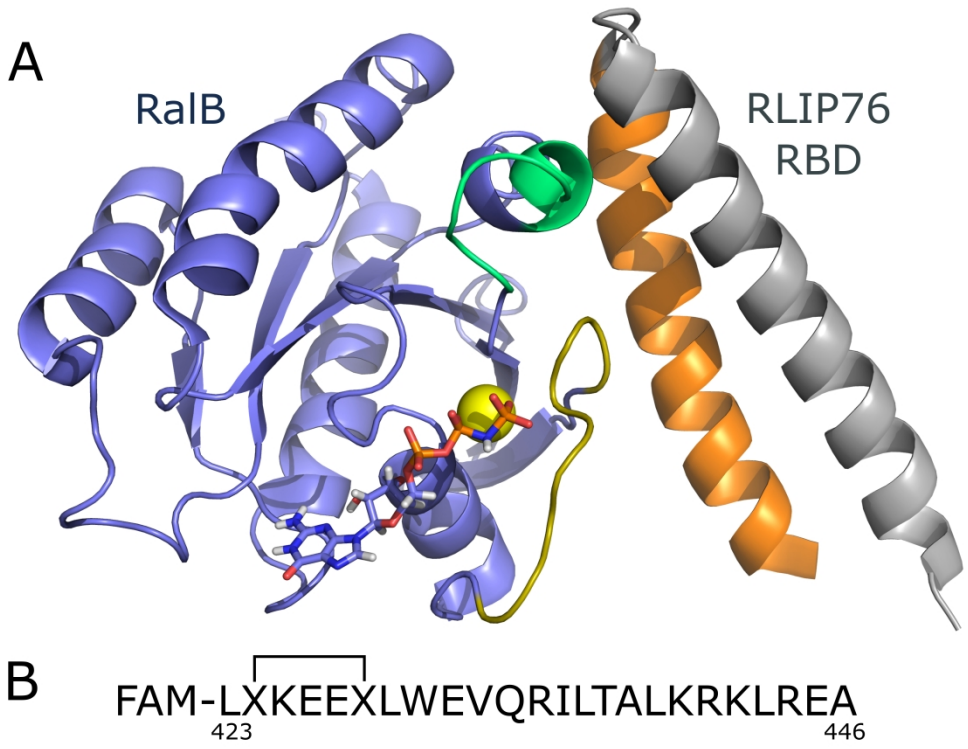

Figure 6

387x298mm (300 x 300 DPI)

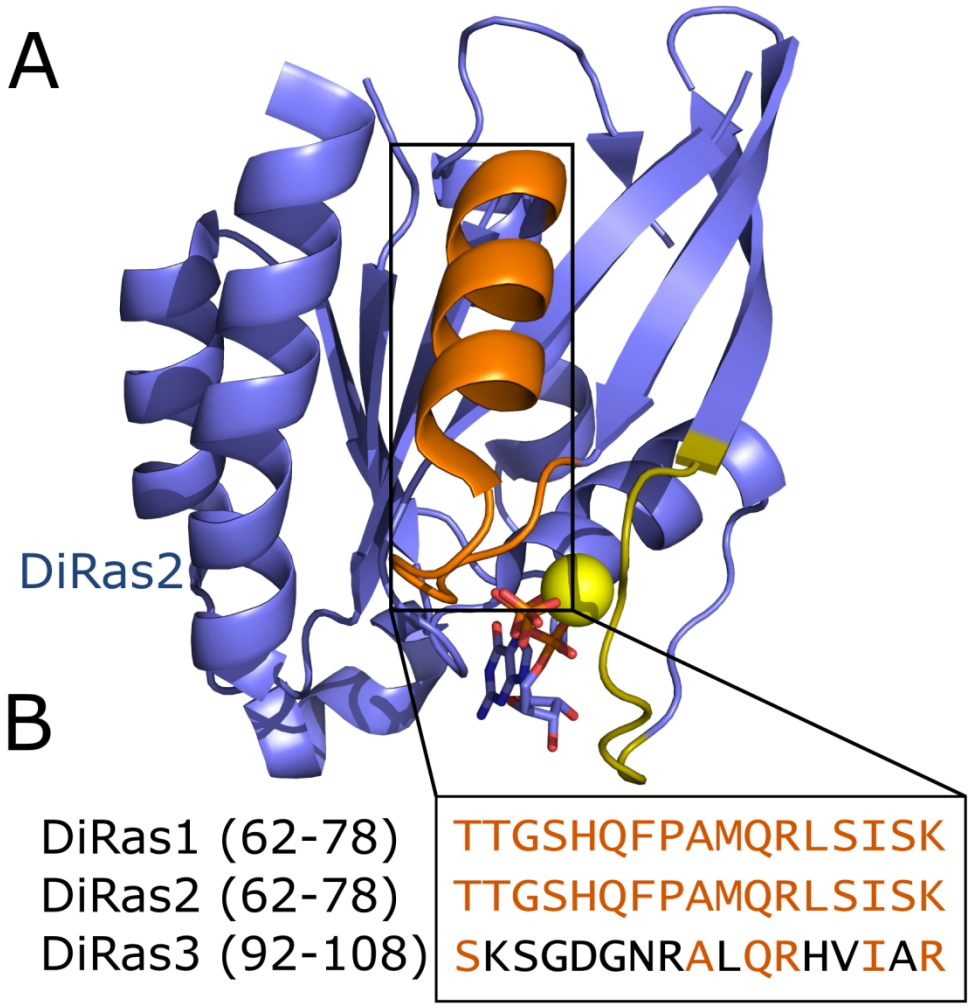

Figure 7

146x150mm (300 x 300 DPI)

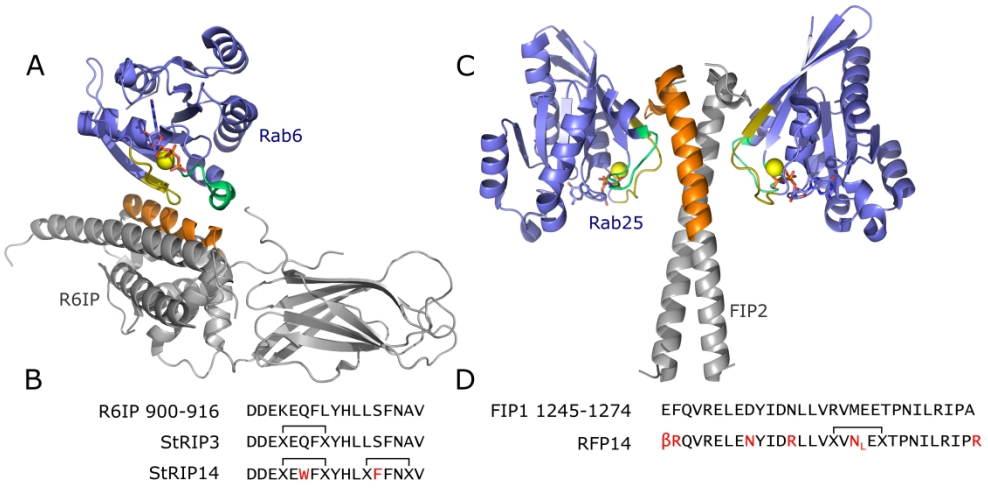

Figure 8

406x203mm (300 x 300 DPI)

Biographies

Catherine A. Hurd obtained an MSci in Medicinal and Biological Chemistry from the University of Nottingham (U.K.) in 2016. She is currently a Ph.D. candidate in the group of Darerca Owen and Helen Mott at the University of Cambridge (U.K.), where her research aims to develop hydrocarbon-stapled peptide inhibitors of protein-protein interactions.

Helen Mott is the Joseph Needham Lecturer in Biochemistry at Gonville and Caius College, and a Senior Lecturer in the Department of Biochemistry, University of Cambridge (U.K.). She obtained a Biochemistry MA and DPhil at the University of Oxford (U.K.). She then joined the Department of Biochemistry and Biophysics at the University of North Carolina at Chapel Hill (U.S.A.) before moving to Cambridge where she was supported by two MRC fellowships prior to becoming a member of the faculty in 2005. Her research focusses on understanding the structure, dynamics and interaction of small GTPases and their effectors.

Darerca Owen is a Senior Lecturer at the University of Cambridge (U.K.) She obtained her BSc (Genetics) and her Ph.D. from the University of Liverpool (U.K.). She joined the Department of Cancer Studies at the University of Birmingham (U.K.) as a post-doctoral research scientist, then moved to the Department of Biochemistry, University of Cambridge, where she became a member of the faculty in 2005. Her research efforts focus on understanding intracellular signalling pathways controlled by small GTPases.

112x110mm (300 x 300 DPI)